

# High stability and electronic structures of noble-metal covered W(111) atom perfect pyramidal tips

Horng-Tay Jeng,\* Hong-Shi Kuo, Ing-Shouh Hwang, and Tien T. Tsong

*Institute of Physics, Academia Sinica, Taipei 11529, Taiwan*

(Received 3 March 2010; published 12 April 2010)

Noble-metal covered W(111) single-atom pyramidal tips (SATs) are artificially created, highly stable atom perfect nanostructures with broad scientific and technological interests. Using first-principles calculations, the binding energy of the topmost atom is found to be nearly identical to the cohesive energy of the metal despite its greatly reduced coordination. This explains the extraordinary high stability of the SATs. In addition, the tip states below  $E_f$  that localize not only in the real space but also in the energy domain is a genetic property of the reduced dimension of the apex of the pyramidal tip structure. The calculated spectral features may also provide a foundation for future scanning tunneling spectroscopy measurements as well as an elemental analysis of surface atoms using SATs in scanning tunneling spectroscopy.

DOI: [10.1103/PhysRevB.81.155424](https://doi.org/10.1103/PhysRevB.81.155424)

PACS number(s): 73.22.-f, 68.37.Vj, 71.15.Nc

## I. INTRODUCTION

A single-atom tip (SAT) is of broad interest both in science and in technology applications. It can be an ideal source of highly phase-coherent particle beams (field electron or gas field ion beams) because of the extremely small atomic size emitting area. The particle beams field emitted from a SAT can be more focused to a very small spot, thus to achieve a very high beam intensity. A SAT can also be used in scanning probe microscopy to achieve atomic resolution<sup>1</sup> which has uncovered many important physics on surfaces of materials. SATs can be prepared in many different ways. Most of them are however hard to reproduce and the tip structures obtained are not thermodynamically stable either. Their usable lifetimes tend to be short that greatly hinder their practical applications. The recent discovery of noble-metal covered W(111) SATs and subsequent improvement of their preparation methods<sup>2</sup> may lead to practical applications of SATs. This type of SATs is confirmed from field ion microscope atom-by-atom analysis to be an atom perfect nanopyramid grown on top of a larger hemispherical base tip. The structure is thermally stable up to a temperature as high as  $>1000$  K, thus can be produced by thermal annealing. Even if SATs are damaged or contaminated, they can be regenerated through a simple annealing. Most importantly, the atomic stacking remains the same for each time which is also completely ordered when compared with the random structure of the traditional SATs.

The discovery of noble-metal covered W(111) SATs and subsequent improvement of their preparation methods<sup>2</sup> may lead to many novel applications of SATs. Recent experimental studies indicate that the electron beams field emitted from these pyramidal SATs can achieve brightness one to four orders of magnitude better than the state-of-the-art electron sources used in current electron microscopes.<sup>3</sup> Full spatial wave coherence (transverse coherence width larger than the beam diameter) of electron beam emitted from an Ir-covered W(111) SAT has also been demonstrated.<sup>4</sup> The full wave coherence and extremely high brightness of the point electron source may open up many new possibilities for electron-beam based techniques such as electron microscopy and

spectroscopy. Also, it has been demonstrated that these SATs can achieved very stable emission of several types of gas ion beams with brightness orders of magnitude higher than that of liquid metal-ion sources used in current focused ion-beam systems.<sup>5</sup> Many novel applications such as ion-beam interferometry and nanodevices with new functions may become possible. Especially the ion interferometry may open a gateway to study fundamental physical principles related to gauge invariance and provide new tests of relativity and gravitation.<sup>6</sup>

The reproducible and well-defined atomic structures of noble-metal covered W(111) SATs will benefit scanning tunneling spectroscopy (STS). In STS measurements, the tip electronic structure is often assumed to be featureless, i.e., the electronic density of states (DOS) does not vary with the energy. Real metal tips that end with only one atom, which is necessary to achieve atomic resolution in scanning tunnel microscope (STM), often possess some features in the electronic density of states. To extract the electronic structure of the sample surface from the STS measurements, it is essential to have detailed information of the tip electronic structure. However, typical STM tips are produced with a random structure and thus the tip electronic structure is largely unknown. The main purposes of this work are to obtain the electronic structures of the atom perfect noble-metal covered W(111) SATs through *ab initio* calculations and to understand the stability of these tips. With the density of states of the probing tip clarified, STS measurements may one day lead to a successful elemental analysis of the sample surface also.

Theoretical calculations of SATs were carried out previously by Lang *et al.*<sup>7</sup> as well as by Gohda *et al.*<sup>8</sup> To simplify the calculations, they combined jellium model with first-principles method. Because of the random structures of the traditional SATs, these calculations are based on fictitious tip structures. Unfortunately their atomic stacking cannot be found in any realistic tip. In this work, full *ab initio* calculations for realistic noble-metal covered W(111) SATs are carried out. The atomic stacking of the SATs for the topmost layers has been determined experimentally, as shown in Fig. 1. The first layer is a noble-metal tip atom, the second layer

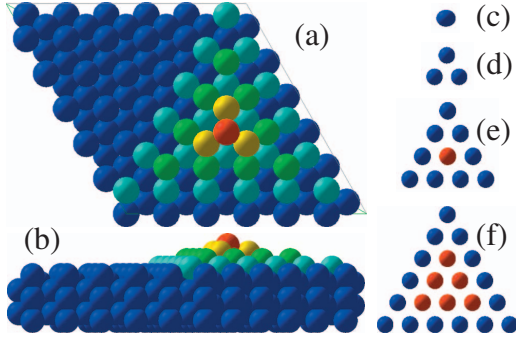


FIG. 1. (Color) Lattice structure of noble-metal covered W(111) single-atom tip. (a) Top and (b) side views of the  $6 \times 6$  three-sided pyramid structure. Red, yellow, green, and light blue spheres denote the first, second, third, and fourth layer atoms of the pyramid. Blue spheres are the tungsten atoms. [(c)–(f)] Atomic model of the topmost four layers of the pyramid. Blue and red balls denote the noble metal and tungsten atoms, respectively.

consists of three noble-metal atoms, the third layer consists of ten atoms with a center tungsten atom surrounded by nine noble-metal atoms, and the fourth layer consists of 21 atoms with center 6 tungsten atoms surrounded by 15 noble-metal atoms. The stacking of the pyramid follows the *ABCABC* stacking of the W(111) slab, except for the mis-stacking of the topmost atom which is located at the same site as the third layer of the pyramid. This mis-stacking results in a direct overlap between the tip atom and the center tungsten atom of the third layer [Figs. 1(c) and 1(e)]. This atomic stacking is consistent with the field ion microscope study of a Pd-covered W(111) SAT by Fu *et al.*<sup>2</sup> They found that the center atom in the third layer required a higher electric field to be evaporated than the surrounding atoms in the same layer, suggesting that the center might be a W atom and the others might be Pd atoms.

## II. COMPUTATIONAL DETAILS

The self-consistent electronic structure calculations are performed using accurate full-potential augmented wave method<sup>9</sup> as implemented in the VASP package<sup>10</sup> within the generalized gradient approximation.<sup>11</sup> The noble-metal covered W(111) SATs are simulated using a  $6 \times 6$  pyramid structure (35 atoms) (Fig. 1) covered with a monolayer of noble-metal atoms over seven layers of W(111) slab (252 atoms)

with a separating vacuum thickness of  $\sim 10$  Å in the super-cell approach. The geometries of the whole nanostructures (287 atoms) are optimized separately for different cover layers (Pd, Pt, Rh, and Ir) over a  $4 \times 4 \times 1$  Monkhorst-Pack *k*-point mesh in the two-dimensional irreducible Brillouin zone using 109 587 plane waves with the cutoff energy of 250 eV.

## III. RESULTS AND DISCUSSION

Experimentally, it has been found that the pyramidal SATs are very stable against annealing, electron field emission, and field evaporation.<sup>2–5</sup> Previous *ab initio* calculations by Chen *et al.*<sup>12</sup> and Che *et al.*<sup>13</sup> have indicated that the experimentally observed formation of the self-assembled pyramidal structure<sup>14,15</sup> is driven by the surface-energy anisotropy-induced {211}-facet formation as the metal films are adsorbed on the W(111) surface. Here we would like to focus on the relative stability or the binding energy of the topmost atom, which is defined as the energy required to remove the topmost atom to the infinity. Table I lists the calculated binding energies for different noble-metal covered W(111) pyramids and the corresponding threshold electric fields for ionizing the topmost atom of the pyramidal SATs measured with field ion microscopy (FIM). The calculated binding energy of 3.49 eV for the Pd-covered tip is the lowest, while the Pt-, Rh-, and Ir-covered tips show larger bindings of 5.62 eV, 5.04 eV, and 5.87 eV, respectively. The obtained binding energies have the same trend as that in the evaporation fields measured in FIM experiments where the threshold electric fields are smallest for Pd (40 V/nm) and larger for Pt(47–49 V/nm), Rh (48 V/nm), and Ir(52–54 V/nm) cases. The relatively low binding energy of the Pd covered tip could be related to the low cohesive energy (CE) of bulk Pd.

The calculated and experimental<sup>16</sup> cohesive energies of related bulk systems are also tabulated for comparison, which indicates that our calculated values are in good agreement with experimental data. Surprisingly, there exists a trend that despite the strongly reduced coordinations of 4 for the tip atom in the pyramidal systems, the calculated binding energies for the topmost noble-metal atoms are quite close to the corresponding fcc bulk cohesive energies with 12 coordinations. For Pd and Pt of the same family, the deviations are unexpectedly small of  $\sim 5\%$  and  $\sim 2\%$ , respectively, while for Rh and Ir of another family, they differ only by  $\sim 15\%$  and  $\sim 20\%$ , respectively. Such high binding energies

TABLE I. Calculated binding energy of the tip atom in the  $6 \times 6$  W(111) pyramid structures with different cover layers and the electric field strengths in FIM for ionizing the tip atom. The calculated and experimental (Ref. 16) CE are also listed for comparison.

	Pd	Pt	Rh	Ir	W
SAT ( $4 \times 4$ )	3.64	5.52	5.14	5.96	
SAT ( $6 \times 6$ )	3.49	5.62	5.04	5.87	
FIM (V/nm)	40	47–49	48	52–54	
CE (Calc., eV)	3.69	5.50	5.90	7.33	8.46
CE (Expt. eV)	3.89	5.84	5.75	6.94	8.90

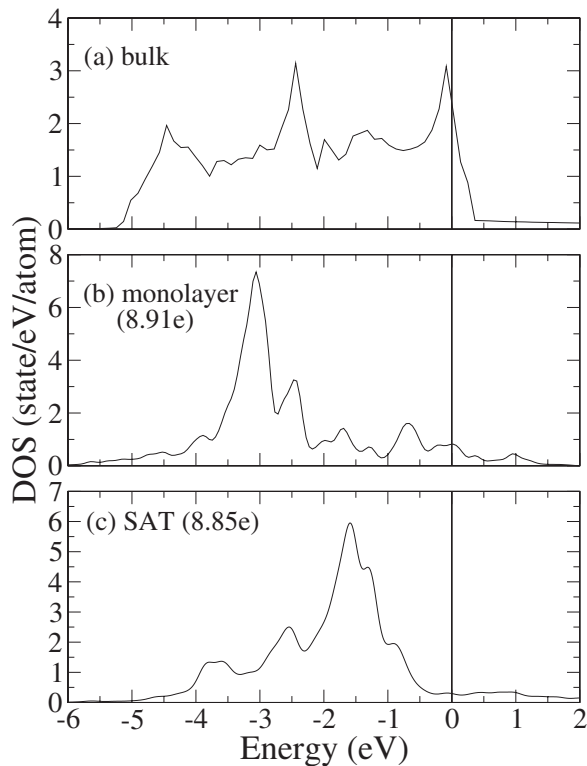


FIG. 2. The origin of the tip states in the Pd-covered single-atom tip. (a) DOS of bulk Pd. (b) DOS of monolayer Pd/W(111). (c) DOS of the tip Pd atom of SAT. The integrated valence charge of monolayer and SAT systems are also indicated in the brackets.

are presumably due to the direct contact between the tip atom and the third layer W atom with a very high cohesive energy, as well as the charge transfer from W to the tip atom as discussed below. The obtained high binding energies, which indicate the high stability of the topmost atoms on the pyramids, can also give a good explanation for the experimental findings as mentioned above.

Figures 2(a)–2(c) show the projected density of states (DOS) of bulk Pd, Pd monolayer on W(111) slab, and tip Pd atom of SAT, respectively. For bulk Pd [Fig. 2(a)], the more or less squarelike Pd  $4d$  band spans from  $\sim 0.5$  eV above the Fermi level ( $E_f$ ) to  $\sim 5.0$  eV below  $E_f$ . Because of the high (12) fcc coordinations with Pd-Pd bond length of 2.75 Å, the bandwidth is as large as  $\sim 5.5$  eV and the intensity is rather uniform throughout the whole Pd  $4d$  band, well indicating the itinerant character of bulk Pd. Although the bond length 2.74 Å of bcc W is close to that of fcc Pd, the W(111) surface is rather open with broken surface bonds, and the shortest Pd-Pd distance in the Pd monolayer over W(111) surface is as large as  $\sim 4.47$  Å. For each overlayer Pd atom, there are only four W nearest-neighbor atoms in the sublayers with bond length similar to W-W bond length. As shown in Fig. 2(b), due to the strongly reduced coordinations and overlaps among wave functions in the surface system, the bandwidth of Pd is drastically reduced to less than 1.5 eV with the peak energy of  $\sim -3.1$  eV lower than the bulk band center at  $\sim -2.5$  eV [Fig. 2(a)]. We note that the relatively lower band center in the Pd monolayer system is due to the contact with the W substrate. This is the reason why in the

calculations, there is nontrivial charge transfer from W to Pd once they coexist in one system. Donated by the four contacting W atoms in this monolayer system, the valence charge of  $8.91e/\text{Pd}$  (indicated in the figure) integrated over the atomic sphere of radius 1.45 Å is relatively high in comparison with the smaller Pd valence charges in the pyramid systems discussed below.

As mentioned previously, the topmost Pd atom of the pyramid is in a direct contact with the center tungsten atom of the third layer. The Pd-W bond length is 1.82 Å without relaxation. After geometry optimization, this tip Pd atom moves outwards stretching the short Pd-W interatomic distance to  $\sim 2.44$  Å, which is still much shorter than the bond length of Pd-Pd (2.75 Å) and W-W (2.74 Å) in bulk systems. In spite of the slightly enhanced interatomic distances of  $\sim 2.90$  Å between the tip atom and the three Pd atoms in the second layer, this short Pd-W bond length indicates a relatively strong bonding, which gives rise to the high binding energy as discussed previously. On the other hand, the topmost Pd atom contacts only one W atom in the pyramid system rather than three W in the monolayer system. As shown in Fig. 2(c), the less contact with the sublayer W results in a much higher peak energy of  $\sim -1.6$  eV with a longer unoccupied tail above  $E_f$  relative to those in the monolayer system [Fig. 2(b)]. Therefore the charge transfer from W to the topmost Pd atom is significantly reduced, leading to a less valence charge of  $8.85e$  in comparison with the higher valence charge of  $8.91e$  in the monolayer case.

The obtained tip state [Fig. 2(c)] localizes not only in the energy domain but also in the real space domain. Figures 3(a) and 3(b) depict the charge contour of the states near  $E_f$  ( $0 \sim -0.4$  eV), and the tip states within  $-1.4 \sim -1.8$  eV of SAT [Fig. 2(c)], respectively. The charge contour of the itinerant states around  $E_f$  shapes into a more or less two-dimensional sheet over the pyramid. In contrast, as can be clearly seen in the figure, the charge densities of the tip states are mainly localized at the tip Pd atom forming the localized peak. Similar behaviors were also reported in the *ab initio* calculations of Al(100) pyramid structure by Gohda *et al.*<sup>8</sup> Most likely this dimension-reduction-induced band localization at the tip atom of the pyramid structure is a generic phenomenon. The narrow localized band with a high intensity would have important implication for the STS measurements using atomically sharp metal tips.

From our FIM studies, the pyramids typically have seven to ten atomic layers. To examine whether or not the  $6 \times 6$  pyramid used in the calculations is large enough for giving a correct, at least qualitatively, description on the larger realistic pyramid observed in experiments, we performed calculations on an even smaller  $4 \times 4$  pyramid with only three layers therein. This is indeed a very strict test on the size effect in this system since all the phenomena presented previously for the  $6 \times 6$  pyramid would be strongly altered if the size effect is important. Figure 4(a) shows the projected DOS of the tip Pd atom of the  $4 \times 4$  and  $6 \times 6$  SATs. It can be clearly seen that the overall band shapes and peak energies of the two pyramids agree well with each other. There is also a localized tip band around 1.8 eV below  $E_f$  with the bandwidth of  $\sim 1.5$  eV in  $4 \times 4$  SAT. The peak energy of the  $4 \times 4$  SAT is only  $\sim 0.2$  eV lower than that of the  $6 \times 6$  SAT. Further-

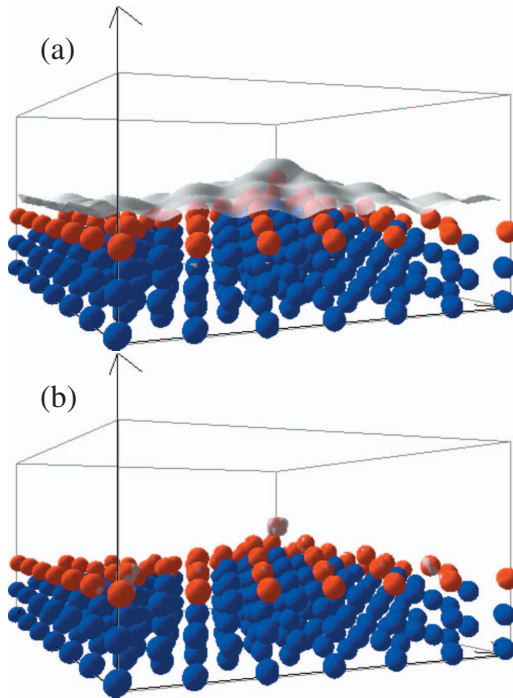


FIG. 3. (Color) (a) Charge contour (gray) of the itinerant states at Fermi level ( $0 \sim -0.4$  eV). (b) Charge contour (gray) of the localized tip states within ( $-1.4 \sim -1.8$  eV). Red and blue spheres denote the Pd cover layer and the W atoms, respectively.

more, the conclusion that the tip state of the  $4 \times 4$  pyramid is similar to the  $6 \times 6$  counterpart remains correct for pyramids covered with different noble-metal monolayers such as Pt, Rh, and Ir as show in Figs. 4(b)–4(d), respectively. Consequently, one can conclude that the formation of the localized tip states and the peak energy are actually local phenomena, being related mainly to the topmost three layers of the pyramid only, therefore a small size  $4 \times 4$  pyramid can already give a correct picture for the localized tip states.

As mentioned above, formation of the localized tip states is a generic phenomenon originated from the reduced dimension of the pyramid structure. However different cover layers do affect the projected DOS of different tip atoms. As shown in Fig. 4(b), the band shapes of Pt covered SATs are similar to those of the Pd covered ones since both Pd and Pt belong to the same family in the periodic table with similar band dispersions in the bulk state. For both the Rh and Ir covered

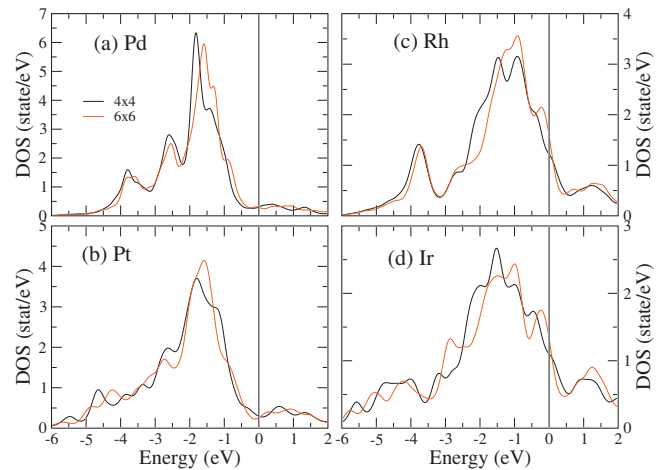


FIG. 4. (Color) Projected density of states of the topmost atom on  $4 \times 4$  (black lines) and  $6 \times 6$  (red lines) pyramids covered with one monolayer (a) Pd, (b) Pt, (c) Rh, and (d) Ir.

cases [Figs. 4(c) and 4(d), respectively], the bandwidths are much larger and the peak intensity are much lower than those of the Pd and Pt ones. This is because of the relatively larger orbital sizes and bandwidths as can be found in bulk Rh ( $\sim 7.5$  eV) and Ir ( $\sim 8.5$  eV).

#### IV. CONCLUSION

Our calculations confirm the surprisingly high stability of noble-metal covered W(111) single-atom pyramidal tips. Very high binding energies of the topmost noble atom in the pyramidal structure are obtained and the origin is related to the direct contact of the topmost atom with the third layer tungsten atom and the charge transfer. We have also systematically investigated the electronic structure of these tips. Results from pyramids with different sizes ( $4 \times 4$  and  $6 \times 6$ ) and different cover layers (Pd, Pt, Rh, and Ir) all reveal that the localized tip band below  $E_f$  is a genetic phenomenon originated from the reduced dimension at the tip of the pyramidal structure. The tip band localizes in both the real space and the energy domain. The calculated spectral features of SATs may provide foundation for future STS measurements with STM.

#### ACKNOWLEDGMENTS

This work was supported by the National Science Council of Taiwan and Academia Sinica. We also thank NCHC, CINC-NTU, and NCTS for technical support.

\*jeng@phys.sinica.edu.tw

<sup>1</sup>G. Binnig, H. Rohrer, C. Gerber, and E. Weibel, *Phys. Rev. Lett.* **49**, 57 (1982); and **50**, 120 (1983).

<sup>2</sup>T. Y. Fu, L. C. Cheng, C. H. Nien, and T. T. Tsong, *Phys. Rev. B* **64**, 113401 (2001); H. S. Kuo, I. S. Hwang, T. Y. Fu, J. Y. Wu, C. C. Chang, and T. T. Tsong, *Nano Lett.* **4**, 2379 (2004).

<sup>3</sup>T. Ishikawa, T. Urata, B. Cho, E. Rokuta, C. Oshima, Y. Terui, H. Saito, A. Yonezawa, and T. T. Tsong, *Appl. Phys. Lett.* **90**, 143120 (2007).

<sup>4</sup>C.-C. Chang, H.-S. Kuo, I.-S. Hwang, and T. T. Tsong, *Nanotechnology* **20**, 115401 (2009).

<sup>5</sup>H.-S. Kuo, I.-S. Hwang, T.-Y. Fu, Y.-H. Lu, C.-Y. Lin, and T. T. Tsong, *Appl. Phys. Lett.* **92**, 063106 (2008).

<sup>6</sup>F. Hasselbach, H. Kiesel, and P. Sonntag, *Decoherence: Theoretical, Experimental, and Conceptual Problems*, Lecture Notes in Physics, edited by P. Blanchard, D. Giulini, E. Joos, C. Kiefer, and I.-O. Stamatescu (Springer-Verlag, Berlin, 2000), Vol. 538, p. 201.

- <sup>7</sup>N. D. Lang, A. Yacoby, and Y. Imry, *Phys. Rev. Lett.* **63**, 1499 (1989).
- <sup>8</sup>Y. Gohda and S. Watanabe, *Phys. Rev. Lett.* **87**, 177601 (2001).
- <sup>9</sup>P. E. Blöchl, *Phys. Rev. B* **50**, 17953 (1994); G. Kresse and D. Joubert, *ibid.* **59**, 1758 (1999).
- <sup>10</sup>G. Kresse and J. Hafner, *Phys. Rev. B* **48**, 13115 (1993); G. Kresse and J. Furthmüller, *Comput. Mater. Sci.* **6**, 15 (1996); *Phys. Rev. B* **54**, 11169 (1996).
- <sup>11</sup>J. P. Perdew, K. Burke, and M. Ernzerhof, *Phys. Rev. Lett.* **77**, 3865 (1996).
- <sup>12</sup>S. P. Chen, *Surf. Sci.* **274**, L619 (1992).
- <sup>13</sup>J. G. Che, C. T. Chan, C. H. Kuo, and T. C. Leung, *Phys. Rev. Lett.* **79**, 4230 (1997).
- <sup>14</sup>K. J. Song, C. Z. Dong, and T. E. Madey, *Langmuir* **7**, 3019 (1991).
- <sup>15</sup>T. E. Madey, J. Guan, C. H. Nien, C. Z. Dong, H. S. Tao, and R. A. Campbell, *Surf. Rev. Lett.* **3**, 1315 (1996).
- <sup>16</sup>See Table 3–2, in C. Kittel, *Introduction to Solid State Physics*, 8th ed. (Wiley, New York, 2005), p. 50.